

## Two Approaches For Direct Torque Control Using a Three-Level Voltage Source Inverter

R. Zaimeddine<sup>1</sup> - E.M. Berkouk<sup>2</sup>

Department of Electrical Engineering  
University of Mouloud Mammeri, Hasnaoua II, Tizi Ouzou  
ALGERIA

**Abstract:** - The object of this paper is to study a new control structure for sensorless induction machine dedicated to electrical drives using a three-level voltage source inverter (VSI). The output voltages of the three-level VSI can be represented by four groups : the zero voltage vectors, the small voltage vectors, the middle voltage vectors and the large voltage vectors in (d , q) plane. Then, the amplitude and the rotating velocity of the flux vector can be controlled freely. Both fast torque and optimal switching logic can be obtained. The selection is based on the value of the stator flux and the torque. Both approaches, classical DTC and fuzzy logic controller, are simulated for a induction motor. The results obtained show superior performances over the FOC one without need to any mechanical sensor.

**Key Words:** - Direct Torque Control, Field Oriented Control, Induction motor, Sensorless Vector Control, Flux Estimators, Switching Strategy Optimisation, Multi-level inverter, Neural-point clamped, fuzzy control.

### 1 Introduction

The rapid development of the capacity and switching frequency of the power semiconductor devices and the continuous advance of the power electronics technology have made many changes in static power converter systems and industrial motor drive areas. The conventional GTO inverters have limitation of their dc-link voltage. Hence, the series connections of the existing GTO thyristors have been essential in realizing high voltage and large capacity inverter configurations with the dc-link voltage [1]. The vector control of induction motor drive has made it possible to be used in applications requiring fast torque control such as traction [2]. In a perfect field oriented control, the decoupling characteristics of the flux and torque are affected highly by the parameter variation in the machine.

This paper describes a control scheme for direct torque and flux control of induction machines fed by a three-level inverter using a switching table. In this method, the output voltage is selected and applied sequentially to the machine through a look-up table so that the flux is kept constant and the torque is controlled by the rotating speed of the stator flux. The direct torque control (DTC) is one of the actively researched control scheme which is based on the decoupled control of flux and torque providing a very quick and robust response with a simple control construction in ac drives [3,4].

### 2 Three-Level Inverter Topology

Fig . 1 shows the schematic diagram of neutral point clamped (NPC) three-level VSI. Each phase of this inverter consists of two clamping diodes, four GTO thyristors and four freewheeling diodes. Table. 1 shows the switching states of this inverter. Since three kinds of switching states exist in each phase, a three level inverter has 27 switching states.

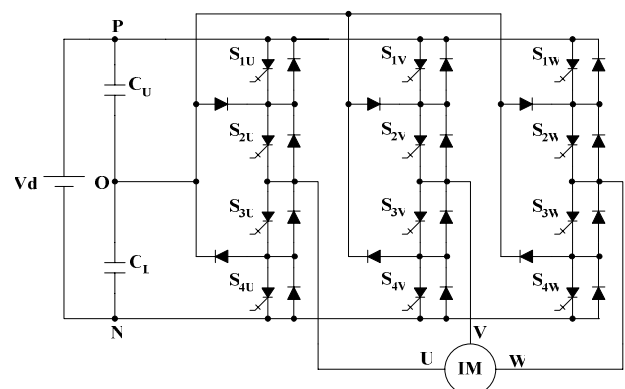


**Fig. 1. Schematic diagram of a three-level GTO inverter**

**Table. 1 Switching states of a three-level inverter**

Switching states	S <sub>1</sub>	S <sub>2</sub>	S <sub>3</sub>	S <sub>4</sub>	V <sub>N</sub>
P	ON	ON	OFF	OFF	V <sub>d</sub>
O	OFF	ON	ON	OFF	V <sub>d</sub> /2
N	OFF	OFF	ON	ON	0

A two-level inverter is only capable to produce six non-zero voltage vectors and two zero vectors [2]. The representation of the space voltage vectors of a three-level inverter for all switching states, according to the magnitude of the voltage vectors, we divide them into four groups : the zero voltage vectors (V<sub>0</sub>), the small voltage vectors (V<sub>1</sub>, V<sub>4</sub>, V<sub>7</sub>, V<sub>10</sub>, V<sub>13</sub>, V<sub>16</sub>), the middle voltage vectors (V<sub>3</sub>, V<sub>6</sub>, V<sub>9</sub>, V<sub>12</sub>, V<sub>15</sub>, V<sub>18</sub>), the large voltage vectors (V<sub>2</sub>, V<sub>5</sub>, V<sub>8</sub>, V<sub>11</sub>, V<sub>14</sub>, V<sub>17</sub>).

The zero voltage vector (ZVV) has three switching states, the small voltage vector (SVV) have two, and both the middle voltage vector (MVV) and the large voltage vector (LVV) have only one [1].

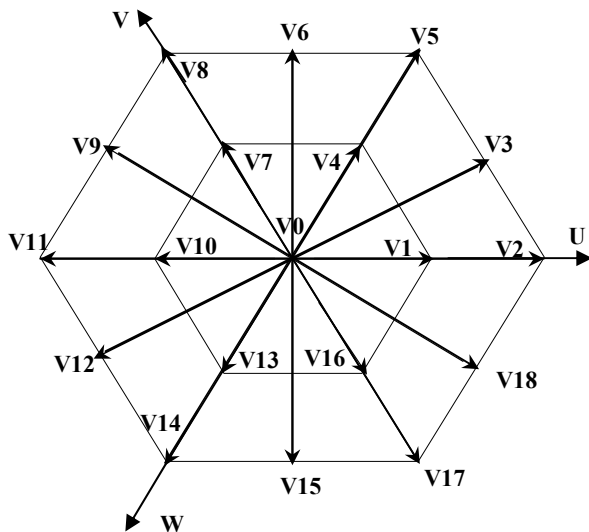


**Fig. 2. Space voltage vectors of a three-level inverter**

### 3 Induction Machine

Torque control of an asynchronous motor can be achieved on the basis of its model developed in a two axes (d, q) reference frame stationary with the stator winding. In this reference frame and with conventional notations, the electrical mode is described by the following equations:

$$\frac{di_{sd}}{dt} = \frac{1}{\sigma T_r L_s} \phi_{sd} + \frac{p\Omega}{\sigma L_s} \phi_{sq} - \frac{1}{\sigma} \left( \frac{1}{T_r} + \frac{1}{T_s} \right) i_{sd} - p\Omega i_{sq} + \frac{1}{\sigma L_s} V_{sd} \quad (1)$$

$$\frac{di_{sq}}{dt} = -\frac{p\Omega}{\sigma L_s} \phi_{sd} + \frac{1}{\sigma T_r L_s} \phi_{sq} - \frac{1}{\sigma} \left( \frac{1}{T_r} + \frac{1}{T_s} \right) i_{sq} + p\Omega i_{sd} + \frac{1}{\sigma L_s} V_{sq} \quad (2)$$

$$\frac{d\phi_{sd}}{dt} = V_{sd} - R_s i_{sd} \quad (3)$$

$$\frac{d\phi_{sq}}{dt} = V_{sq} - R_s i_{sq} \quad (4)$$

The mechanical mode associated to the rotor motion is described by :

$$J \frac{d\Omega}{dt} = \Gamma_{em} - \Gamma_r(\Omega) \quad (5)$$

$\Gamma_r(\Omega)$  and  $\Gamma_{em}$  are respectively the load torque and the electromagnetic torque developed by the machine.

### 4 Stator Flux and Torque Estimation

Basically, DTC schemes require the estimation of the stator flux and torque. The stator flux evaluation can be carried out by different techniques depending on whether the rotor angular speed or (position) is measured or not. For sensorless application, the “voltage model” is usually employed [5].

The stator flux can be evaluated by integrating from the stator voltage equation.

$$\phi_s(t) = \int (V_s - R_s I_s) dt \quad (6)$$

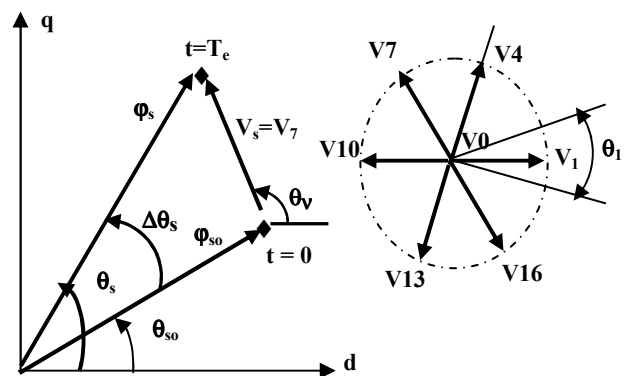


**Fig. 3. Flux deviation**

This method is very simple requiring the knowledge of the stator resistance only. The effect of an error in  $R_s$  is usually quite negligible at high excitation frequency but becomes more serious as the frequency approaches zero [5].

The deviation obtained as the end of the switching period  $T_e$  can be approached by the first order Taylor Seri as below.

$$\begin{aligned} \Delta\varphi_s &\approx V_s \cdot T_e \cdot \cos(\theta_v - \theta_s) \\ \Delta\theta_s &\approx T_e \cdot \frac{V_s \cdot \sin(\theta_v - \theta_s)}{\varphi_{so}} \end{aligned} \quad (7)$$

Considering the combination of states of switching functions  $S_u, S_v, S_w$ . Fig.3 shows the adequate voltage vector selection we can increase or decrease the stator flux amplitude and phase to obtain the required performances. The electric torque is estimated from the flux and current information as [2]:

$$\Gamma_{em} = p(i_{sq}\varphi_{sd} - i_{sd}\varphi_{sq}) \quad (8)$$

### 5 Conventional Direct Torque Control

Fig. 4. shows a block diagram of the DTC scheme. The reference values of flux,  $\varphi_s^*$ , and torque,  $\Gamma_{em}^*$ , are compared to their actual values and the resultant errors are fed into a two level comparator of flux and torque.

The stator flux angle,  $\theta_s$  is calculated by :

$$\theta_s = \arctan \frac{\varphi_{sq}}{\varphi_{sd}} \quad (9)$$

And quantified into 6 levels depending on which sector the flux vector falls into. Different switching strategies can be employed to control the torque according to whether the flux has to be reduced or increased.

Each strategy affect the drive behavior in terms of torque and current ripple, switching frequency and two or four-quadrant operation capability.

Assuming the voltage drop  $R_s i_s$  small, the head of the stator flux  $\varphi_s$  moves in the direction of stator voltage  $V_s$  at a speed proportional to the magnitude of  $V_s$  according to

$$\Delta\varphi_s = V_s T_e \quad (10)$$

The switching configuration is made step by step, in order to maintain the stator flux and torque within limits of two hysteresis bands. Where  $T_e$  is

the period in which the voltage vector is applied to stator winding. Selecting step by step the voltage vector appropriately, it is then possible to drive  $\varphi_s$  along a prefixed track curve.

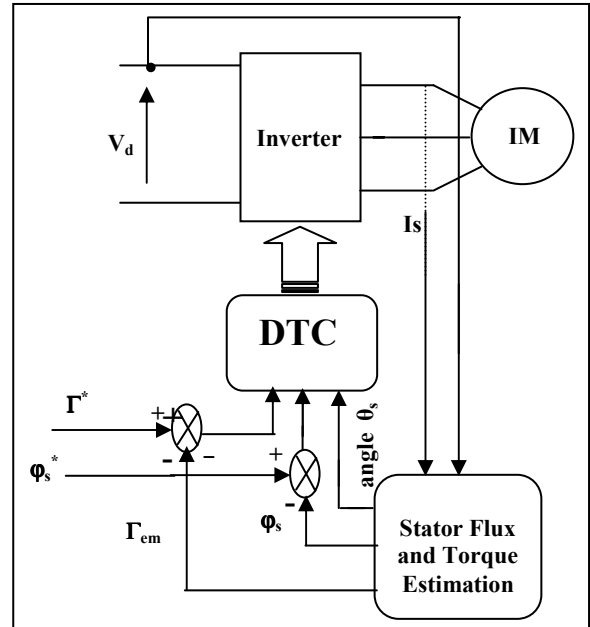


Fig. 4. Block diagram of direct torque control

Assuming the stator flux vector lying in the  $k$ -th sector ( $k=1,2,3,4,5,6$ ) of the  $(d, q)$  plane, in the case of three-level inverter, to improve the dynamic performance of DTC at low speed and to allow four-quadrant operation, it is necessary to involve the voltage vectors  $V_{K-1}$  and  $V_{K-2}$  in torque and flux control. In the following,  $V_{K-1}$  and  $V_{K-2}$  will be denoted "backward" voltage vectors in contraposition to "forward" voltage vectors utilised to denote  $V_{K+1}$  and  $V_{K+2}$ . A simple strategy which makes use of these voltage vectors is shown in table. 2. The conventional DTC has been studied, [6].

Table.2 Selection strategy for four-quadrant operation

		$\Gamma_{em} \uparrow$	$\Gamma_{em} \downarrow$
$\varphi_s \uparrow$		$V_{K+1}$	$V_{K-1}$
$\varphi_s \downarrow$		$V_{K+2}$	$V_{K-2}$

For steady operating conditions, equations (8) describing the machine torque can be transformed to a sinus function :

$$\Gamma_{elmo} = \Gamma_{maxo} \cdot \sin 2\gamma_o \quad (11)$$

$\Gamma_{\max o}$  and  $\gamma_o$  are equation respectively torque and the difference angle between stator and rotor flux vectors.

$$\Gamma_{\max o} = p \cdot \frac{1-\sigma}{2 \cdot \sigma \cdot L_s} \cdot \varphi_{so}^2 \quad ; \quad \gamma_o = \theta_{so} - \theta_{ro} \quad (12)$$

Equations (11) and (12) are established with the assumption that stator flux and rotor closed values in steady state. For disturbed states, the stator flux angle  $\theta_s$  has in practice a fast dynamic mode as compared to the rotor flux angle  $\theta_r$ . If these two assumptions are hold the effect of stator vector voltage on the machine torque can be expressed by the first order Taylor expansion as below :

$$\Delta \Gamma_{elm} \approx K_{\varphi} \cdot \Delta \varphi_s + K_{\theta} \cdot \Delta \theta_s \quad (13)$$

The sensitivity coefficients  $K_{\varphi}$  et  $K_{\theta}$  are defined by :

$$\begin{cases} K_{\varphi} = \frac{d\Gamma_{elm}}{d\varphi_s} = \frac{2}{\varphi_{so}} \cdot \Gamma_{elmo} \\ K_{\theta} = \frac{d\Gamma_{elm}}{d\theta_s} = 2 \cdot \Gamma_{\max o} \cdot \cos 2\gamma_o \end{cases} \quad (14)$$

linking equations (7), (13) and (14) leads to :

$$\begin{aligned} \Delta \Gamma_{elm} = & 2 \cdot \frac{V_s \cdot T_e}{\varphi_{so}} \cdot \Gamma_{elmo} \cdot \cos(\theta_v - \theta_{so}) \\ & + \frac{2 \cdot V_s \cdot T_e}{\varphi_{so}} \cdot \sqrt{\Gamma_{\max o}^2 - \Gamma_{elmo}^2} \cdot \sin(\theta_v - \theta_{so}) \end{aligned} \quad (15)$$

This shows the feasibility torque control by a well selected vectors voltage  $\bar{V}_s$  [7].

According to this strategy, the stator flux vector is required to rotate in both positive and negative directions. By this, even at very low shaft speed, large negative values of rotor angular frequency can be achieved, which are required when the torque is to be decreased very fast. Furthermore, the selection strategy represented in Table. II allows good flux control to be obtained even in the low speed range. However, the high dynamic performance which can be obtained utilising voltage vectors having large components tangential to the stator vector locus implies very high switching frequency.

## 6 Switching Strategy Proposed

A switching table is used to select the best output voltage depending on the position of the stator flux and desired action on the torque and stator flux. The flux position in the (d , q) plane is quantified in six sectors. Alternative tables exist for specific operation mode. The switching table for the case of a two-level inverter developed by I. Takahashi [2] , it is easily possible to expand the optimal vector selection to include the larger number of voltage vectors produced by three-level inverter. The appropriate vector voltage is selected in the order to reduce the number of commutation and the level of steady-state ripple.

For flux control, let the variable  $E_{\varphi}$  ( $E_{\varphi} = \varphi_s^* - \varphi_s$ ) be located in one of the three regions fixed by the constraints :

$$E_{\varphi} < E_{\varphi \min} , E_{\varphi \min} \leq E_{\varphi} \leq E_{\varphi \max} , E_{\varphi} > E_{\varphi \max} .$$

The switable flux level is then bounded by  $E_{\varphi \min}$  and  $E_{\varphi \max}$ . The flux control is made by two-level hysteresis comparator. Three regions for flux location are noted, flux as in fuzzy control schemes, by  $E_{\varphi n}$  (negative),  $E_{\varphi z}$  (zero) and  $E_{\varphi p}$  (positive). A high level performance torque control is required. To improve the torque control let of the mismath  $E_{\Gamma}$  ( $E_{\Gamma} = \Gamma_{em}^* - \Gamma_e$ ) to belong to one of the five regions defined by the constraints :

$$E_{\Gamma} < E_{\Gamma \min 2} , E_{\Gamma \min 2} \leq E_{\Gamma} \leq E_{\Gamma \min 1} , E_{\Gamma \min 1} \leq E_{\Gamma} \leq E_{\Gamma \max 1} , E_{\Gamma \max 1} \leq E_{\Gamma} \leq E_{\Gamma \max 2} \text{ and } E_{\Gamma \max 2} < E_{\Gamma} .$$

The five regions defined for torque location are also noted, as in fuzzy control schemes, by  $E_{\Gamma nl}$  (negative large),  $E_{\Gamma ns}$  (negative small),  $E_{\Gamma z}$  (zero),  $E_{\Gamma ps}$  (positve small),  $E_{\Gamma pl}$  (positive large). The torque is then controlled by an hysteresis comparator built with two lower bounds and two upper known bounds [6].

## 7 The Fuzzy Controller

Flux error “ $E_{\varphi}$ ” torque error “ $E_{\Gamma}$ ” and flux position “ $\theta_s$ ” are used as inputs to the fuzzy controller the inverter switchnig state “n” is the output of the controller. The three input variables are divided into their fuzzy segments. The membre of fuzzy segments are chosen to have maximum control with a minimum number of rules. The grade of member distribution of input variables into their fuzzy segments is schows in Fig.5 [8].

The control rule is described by the input variables  $E_\phi$ ,  $E_\Gamma$  and  $\theta$  and the control variable  $n$  as :

$R_i$  : if  $E_\phi$  is  $A_i$  ,  $E_\Gamma$  is  $B_i$  and  $\theta$  is  $C_i$  than  $n$  is  $N_i$

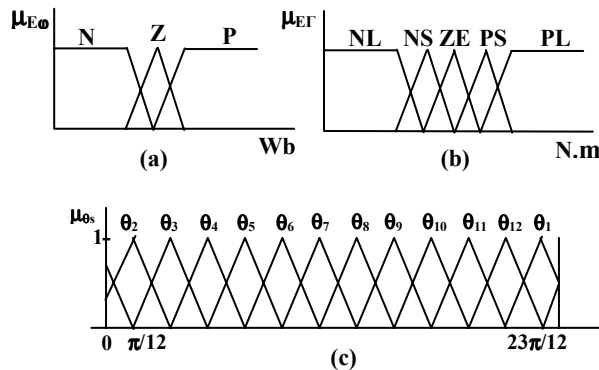


Fig. 5. Membership distribution of fuzzy variables

### 8 Switching Strategy for Fuzzy Controller

The rules are formulated using the vector diagram for direct torque control and flux control of induction machine shows in Fig. 3. The switching strategy in the order of the sector  $\theta_s$ , is illustrate by each tables. The flux and torque control by vector voltage has in nature a desecrate behavior. In fact, we can easily verify that the same vector could be adequate for a set of value of  $\theta_s$  . The number of sectors should be as large as possible to have an adequate decision.

For this reason, we propose a new approach for direct torque control using a three-level inverter based on twelve regular sectors noted by  $\theta_1$  to  $\theta_{12}$  .

A switching table is used to select the best output voltage depending on the position of the stator flux and desired action on the torque and stator flux. It is possible to expand the optimal vector selection to include the larger number of regular sectors and fuzzy segments of input variables.

$\theta_1$				$\theta_2$			
$E_\Gamma \backslash E_\phi$	P	Z	N	$E_\Gamma \backslash E_\phi$	P	Z	N
PL	5	4	8	PL	5	4	8
PS	3	4	6	PS	6	7	9
ZE	0	0	0	ZE	0	0	0
NS	18	0	15	NS	18	0	15
NL	17	13	14	NL	2	16	17

$\theta_3$				$\theta_4$			
$E_\Gamma \backslash E_\phi$	P	Z	N	$E_\Gamma \backslash E_\phi$	P	Z	N
PL	8	7	11	PL	8	7	11
PS	6	7	9	PS	9	10	12
ZE	0	0	0	ZE	0	0	0
NS	3	0	18	NS	3	0	18
NL	2	16	17	NL	15	1	2

$\theta_5$				$\theta_6$			
$E_\Gamma \backslash E_\phi$	P	Z	N	$E_\Gamma \backslash E_\phi$	P	Z	N
PL	11	10	14	PL	11	10	14
PS	9	10	12	PS	12	13	15
ZE	0	0	0	ZE	0	0	0
NS	6	0	3	NS	6	0	3
NL	5	1	2	NL	8	4	5

$\theta_7$				$\theta_8$			
$E_\Gamma \backslash E_\phi$	P	Z	N	$E_\Gamma \backslash E_\phi$	P	Z	N
PL	14	13	17	PL	14	13	17
PS	12	13	15	PS	15	16	18
ZE	0	0	0	ZE	0	0	0
NS	9	0	6	NS	9	0	6
NL	8	4	5	NL	11	7	8

$\theta_9$				$\theta_{10}$			
$E_\Gamma \backslash E_\phi$	P	Z	N	$E_\Gamma \backslash E_\phi$	P	Z	N
PL	17	16	2	PL	17	16	2
PS	15	16	18	PS	18	1	3
ZE	0	0	0	ZE	0	0	0
NS	12	0	9	NS	12	0	9
NL	11	7	8	NL	14	10	11

$\theta_{11}$				$\theta_{12}$			
$E_\Gamma \backslash E_\phi$	P	Z	N	$E_\Gamma \backslash E_\phi$	P	Z	N
PL	2	1	5	PL	2	1	5
PS	18	1	3	PS	3	4	6
ZE	0	0	0	ZE	0	0	0
NS	15	0	12	NS	15	0	12
NL	14	10	11	NL	17	13	14

There is a total of 180 rules, the control rule is described and developed using Mamdani's minimum operation rule [8].

$$\mu'_{Ni}(n) = \min(\alpha_i, \mu_{Ni}(n)) \tag{16}$$

$$\alpha_i = \min(\mu_{Ai}(E_\phi), \mu_{Bi}(E_\Gamma), \mu_{Ci}(\theta_s)) \tag{17}$$

where  $\mu_A$ ,  $\mu_B$ ,  $\mu_C$ , and  $\mu_N$  are membership function of sets A, B, C and N of the variables  $E_\phi$ ,  $E_\Gamma$ ,  $\theta$  and  $n$  respectively. Thus the member function  $\mu_N$  of the output  $n$  (i.e., the Nth rule) is point wise given by :

$$\mu_{Ni}(n) = \max_{i=1}^{180} (\mu'_{Ni}(n)) \tag{18}$$

The maximum criterion method is used for defuzzification, the outputs are crisp in this case because the flux and torque control by vector voltage has in nature a desecrate behavior.

$$\mu_{Nout}(n) = \max_{N=1}^{19} (\mu_N(n)) \tag{19}$$

The fuzzy output which has the maximum possibility distribution, is used as control output. Then output =  $N_{out}$

### 9 The Simulation Results

The validity of the proposed DTC scheme for three-level voltage source inverter is proved by the simulation results using Matlab-Simulink.

The parameters of motors are given in the Appendix. The used flux and torque mismatches for the approach are expressed in percent with respect to th flux and torque reference values.

$$E_{\varphi_{max}} = 3\% , E_{\varphi_{min}} = -3\% , \\ E_{\Gamma_{min1}} = -0.8\% , E_{\Gamma_{min2}} = -3\% , E_{\Gamma_{max1}} = 0.8\% , E_{\Gamma_{max2}} = 3\% .$$

The simulation results illustrates both the steady state and the transient performance of the proposed torque control scheme. However, the machine has been supposed to run at load.

$$\Gamma_r = \left( \frac{\Gamma_{em}}{\Omega_{ref}} - K_f \right) \cdot \Omega \quad (20)$$

Fig.6 shows the phase current and flux for steady state operation at 9 N.m with 0.9 Wb. The wave form of the stator current is closed to a sinusoidal signal. The trajectory of the flux in the case of a fuzzy controller is nearly a circle compared to the flux response in conventional DTC control.

Fig.7 shows the torque reverse response from + 9 N.m to - 9 N.m and flux for 0.9 Wb. The output torque reaches the new reference torque in about 3ms, fast torque response is obtained.

The steady state behavior of the fuzzy controller is given in Fig. 8. Very low flux and torque ripple in the case of the new approach is observed.

The phase current generated by the three-level inverter have low harmonic components. Fig.9. shows the current harmonics with the new approach (5 % THD).

It is concluded that the proposed control produces better results for transient and steady state operation then the classical control.

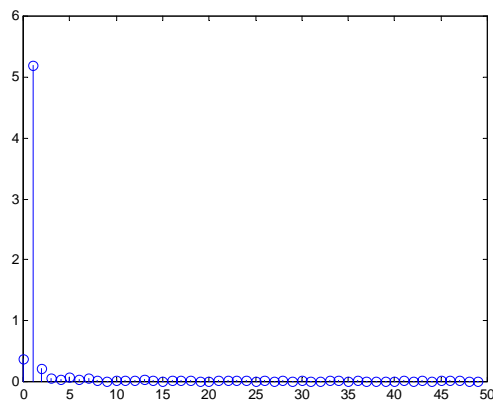


Fig. 9 : Current harmonics Isa1 for fuzzy controller

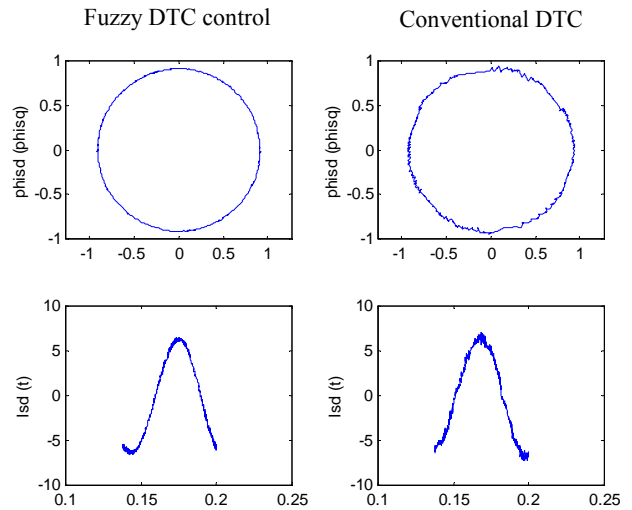


Fig. 6 : Vector flux locus and current response

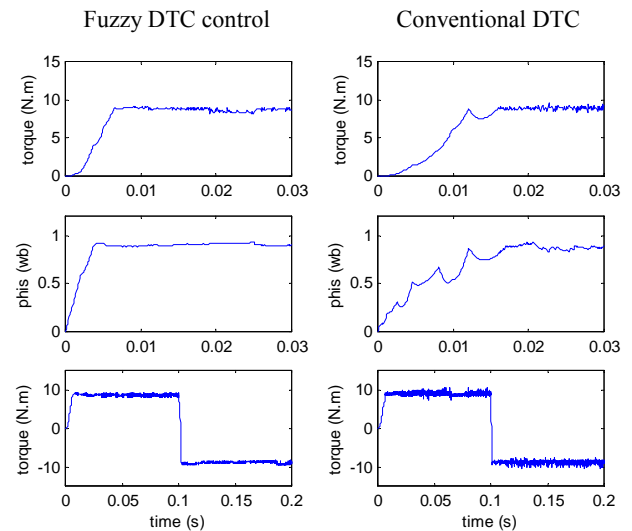


Fig. 7 : Torque and flux response

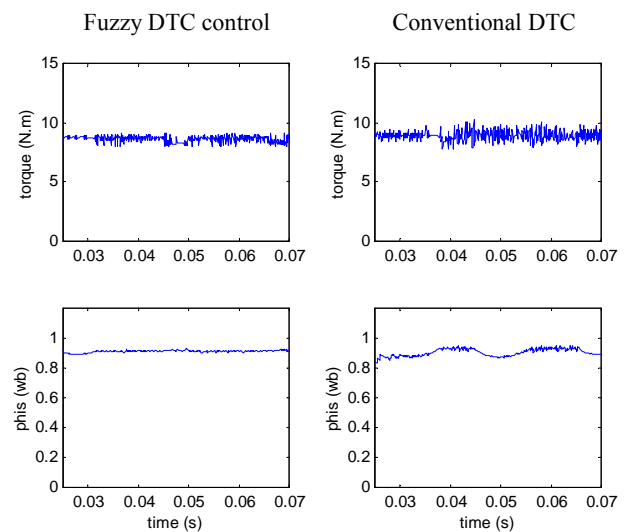


Fig. 8 : Torque response and flux

## 10 Conclusions

The direct torque control DTC was introduced to give a fast and good dynamic torque and can be considered as an alternative to the field oriented control FOC technique. It is concluded that the proposed control produces better results for transient and the steady state operation than the conventional control. However, the two approaches indicate a good regulation.

In this paper, a DTC systems using three-level GTO voltage source inverter is presented it is suitable for high-power and high-voltage applications. We enhance the DTC approach by introducing fuzzy logic controller. From the analysis of these results establish the following remarks :

The fuzzy logic approach has a fast torque and flux response as compared to the conventional DTC.

The stator current wave form is more close to the suitable sinusoidal signal in the fuzzy controller case.

In fact, on line application and control schemes including parameters correction is suitable used the fuzzy logic criterion. From this analysis high dynamic performance, good stability and precision are achieved.

Two problems usually associated with DTC drives which are based on hysteresis comparators are: variable switching frequency and inaccurate stator flux estimation which can degrade the drive performance.

## Appendix

### List of the used notations

$L$  : magnetizing Inductance

$L_m$  : mutual inductance ;

$V$  : voltage

$i$  : current

$\phi$  : flux

$R$  : resistance

$\Gamma_{em}$  : electromagnetic torque

$J$  : rotor inertia

$P$  : number of pairs of poles

$\omega_s$  : statoric pulsation

$V_d$  : dc-link voltage

$K_f$  : friction Coefficient

$T_e$  : sampling time

$E$  : error of the variables

$E$  : error of the variables.

$\omega_r$  : electric rotor speed ;  $\Omega = p \omega_r$ .

$\sigma$  : leakage coefficient,  $\sigma = 1 - \frac{L_m^2}{L_s \cdot L_r}$

$T_r$  : rotor time response,  $T_r = \frac{L_r}{R_r}$

$T_s$  : stator time response,  $T_s = \frac{L_s}{R_s}$

### Induction motors parameters

Rated power : 1.5 kW; Rated voltage : 220 V; Rated speed : 1420 rpm; Rated frequency : 50 Hz; Rated current : 3.64 A (Y) et 6.31 ( $\Delta$ ); Stator resistance : 4.85  $\Omega$ ; Rotor resistance : 3.805  $\Omega$ ; Stator inductance : 0.274 H; Rotor inductance : 0.274 H; Magnetizing Inductance : 0.258 H; Number of poles : 2 ; Rotor inertia : 0.031 Kg.m<sup>2</sup>; Friction Coefficient : 0.008 N.m.s/rd ;  $V_{dc} = 514$  v ;  $T_e = 100$   $\mu$ s;

### References:

- [1] Y.H. Lee, B.S. Suh, and D.S. Hyan, *A novel PWM scheme for a three-level voltage source inverter with GTO thyristors*, IEEE Trans. on Ind. Appl, vol. 33 2, March\April 1996, pp. 260-268.
- [2] I. Takahashi and T. Noguchi, *A new quick-response and high-efficiency control strategy of an induction motor*, IEEE Trans. on IA, vol. 22, No. 5, Sept\Octo 1986, pp. 820-827.
- [3] J.C. Trounce, S.D. Round, and R..M. Duke, *Comparison by simulation of three-level induction motor torque control schemes for electrical vehicle applications*, Proc. of international power engineering conference, vol. 1, May 2001, pp. 294-299.
- [4] WU. Xuezh, and L. Huang, *Direct torque control of three-level inverter using neural networks as switching vector selector*, IEEE IAS, annual meeting, 30 September\ 04 October 2001.
- [5] D. Casadei, G. Grandi, G. Serra, and A. Tani, *Switching strategies in direct torque control of induction machines*, ICEM 94, vol. 2, 1994, pp.204-209.
- [6] R. Zaimeddine, and E.M. Berkouk, *A Novel DTC scheme for a three-level voltage source inverter with GTO thyristor*, SPEEDAM 2004, Symposium on power electronics, electrical drives, automation & Motion, June, vol. 2, June, 16<sup>th</sup>-18<sup>th</sup> 2004, pp. F1A-9-F1A-12.
- [7] F. Bacha, A. sbai, and R. Dhifau, *Tow Approaches For Direct Torque Control of an Induction Motor*, CESA Symposium on control, vol. 1, March 1998, pp. 562-568.
- [8] S.A. Mir, M.E. Elbuluk and D.S Zinger *fuzzy implementation of direct self control of induction machines*, IEEE Trans. on IA, vol. 30, No. 3, May\June 1994, pp. 729-735.